Open

Oncogene (2012) **31,** 4527–4535

www.nature.com/onc

ORIGINAL ARTICLE

A novel function for platelet-derived growth factor D: induction of osteoclastic differentiation for intraosseous tumor growth

W Huang[1,3], Y Fridman[1,3,4], RD Bonfil[1,2], CV Ustach[1], MK Conley-LaComb[1], C Wiesner[2,5], A Saliganan[2], ML Cher[1,2] and H-RC Kim[1]

Although increasing evidence suggests a critical role for platelet-derived growth factor (PDGF) receptor β (β-PDGFR) signaling in prostate cancer (PCa) progression, the precise roles of β-PDGFR and PDGF isoform-specific cell signaling have not been delineated. Recently, we identified the PDGF-D isoform as a ligand for β-PDGFR in PCa and showed that PDGF-D is activated by serine protease-mediated proteolytic removal of the CUB domain in a two-step process, yielding first a hemidimer (HD) and then a growth factor domain dimer. Herein, we demonstrate that the expression of PDGF-D in human PCa LNCaP cells leads to enhanced bone tumor growth and bone responses in immunodeficient mice. Histopathological analyses of bone tumors generated by PDGF-D-expressing LNCaP cells (LNCaP-PDGF-D) revealed osteolytic and osteoblastic responses similar to those observed in human PCa bone metastases. Importantly, we discovered a novel function of PDGF-D in the regulation of osteoclast differentiation, independent of the RANKL/RANK signaling axis. Although both PDGF-B and -D were able to activate β-PDGFR, only PDGF-D was able to induce osteoclastic differentiation *in vitro*, and upregulate the expression and nuclear translocation of nuclear factor of activated T cells 1, a master transcription factor for osteoclastogenesis. Taken together, these results reveal a new function of PDGF-D as a regulator of osteoclastic differentiation, an activity critical for the establishment of skeletal metastatic deposit in PCa patients.

Oncogene (2012) **31,** 4527–4535; doi:10.1038/onc.2011.573; published online 12 December 2011

Keywords: prostate cancer; bone responses; osteoclastic differentiation; PDGF-D

INTRODUCTION

The 'seed and soil' hypothesis is often invoked to address cellular and molecular mechanisms underlying the tendency of prostate cancer (PCa) to metastasize to bone. Cancer cells, upon their arrival in the bone marrow, perturb the delicate homeostatic balance of the bone marrow microenvironment by activating proteolytic cascades and growth factor signaling networks.[1] Tumor-mediated bone responses include increased osteoclast differentiation, leading to bone destruction and new bone formation. Growth-promoting factors released from the metabolized bone matrix during osteoclastic bone resorption are thought to provide a favorable microenvironment for tumor cell proliferation, creating a positive feedback signaling loop. Thus, it is important to identify PCa cell-initiated signaling axes critical for tumor–bone stromal interactions for more in-depth understanding of PCa bone metastasis.

The platelet-derived growth factor (PDGF) family, known as a mesenchymal growth factor, consists of four members, PDGF-A, -B, -C and -D. PDGFs have critical roles in epithelial–stromal communication during physiological or pathological conditions.[2] These interactions are often initiated by PDGF receptor signaling in stroma that is activated by the PDGF ligand produced by epithelial cells. While PDGF-A and -B are secreted as active growth factor dimers and readily activate their cognate receptors, α-PDGFR and β-PDGFR, the newly discovered PDGF family members PDGF-C and PDGF-D are secreted as latent homodimers containing the N-terminal CUB domain and the C-terminal growth factor domain (GFD). Removal of the CUB domain is required for PDGF-C and -D to activate α-PDGFR and β-PDGFR, respectively.[3–5] Recently, we showed that PDGF-D is activated by serine proteases in a two-step process, creating a hemidimer (HD) followed by a GFD dimer (GFD-D). Proteolytic cleavage of the hinge domain in one chain generates a HD containing one full-length and one GFD, and the subsequent cleavage of the hinge domain in the other chain results in GFD-D.[6]

Increasing evidence indicates a critical role for β-PDGFR signaling in PCa bone metastasis. Amplification of the conserved domains of tyrosine kinase receptors using degenerate primers identified PDGFRs as the most commonly amplified transcripts from pooled aspirate specimens of PCa bone metastases.[7] Another study revealed that β-PDGFR is one of five genes that predict recurrence after prostatectomy.[8] Indeed, a majority of PCa tissues express β-PDGFR at both primary and metastasized sites in the bone, as determined by immunohistochemical analysis.[9] Consistent with the potential oncogenic activity of PDGF signaling in PCa progression, investigators have reported the therapeutic potential of targeting PDGF/PDGFR axis in clinical trials of hormone refractory PCa.[10,11] However, it was unclear as to how β-PDGFR is activated, because the expression of PDGF-B, thought for more than two decades to be the sole ligand for β-PDGFR, has not been found to be elevated in PCa. Our recent immunohistochemical analysis of human PCa specimens showed that increased PDGF-D expression is associated with increased Gleason scores and tumor stage.[6] Importantly, we previously showed that

[1]Department of Pathology, Barbara Ann Karmanos Cancer Institute, Wayne State University School of Medicine, Detroit, MI, USA and [2]Department of Urology, Barbara Ann Karmanos Cancer Institute, Wayne State University, School of Medicine, Detroit, MI, USA. [3]These authors contributed equally to this work. [4]Current address: Department of Internal Medicine, University of Michigan, 1500 E. Medical Center Dr. SPC 5052, 2F208UH, Ann Arbor, MI 48109, USA. [5]Current address: Department of Urology, J.W. Goethe University, Theodor-Stern-Kai 7, 60590 Frankfurt, Germany. Correspondence: Professor H-R C Kim, Department of Pathology, Barbara Ann Karmanos Cancer Institute, Wayne State University School of Medicine, 540 E. Canfield, Detroit, MI 48201, USA. E-mail: hrckim@med.wayne.edu
Received 15 November 2010; revised and accepted 10 November 2011; published online 12 December 2011

increased PDGF-D/β-PDGFR signaling accelerates the early onset of subcutaneous tumors formed by LNCaP PCa cells in severe combined immunodeficient mice, and drastically enhances cancer cell invasion into the surrounding stroma,[12] demonstrating a potential oncogenic activity of PDGF-D in PCa.

In this study, we wished to determine the functional significance of tumor-derived PDGF-D in tumor-induced bone reactions as well as the establishment and expansion of skeletal metastatic deposits. Here, we show that PDGF-D expression in LNCaP cells facilitates intraosseous tumor growth and leads to both osteolytic and osteoblastic responses. Importantly, we demonstrate that recombinant PDGF-D directly stimulates osteoclast differentiation *in vitro*, independent of the receptor activator of nuclear factor *k*B ligand (RANKL) signaling axis. Although both PDGF-B and -D are able to activate β-PDGFR, PDGF-D, but not PDGF-B, induces multinucleation and osteoclast differentiation *in vitro*. PDGF-D-specific signal transduction results in increased expression and nuclear translocation of nuclear factor of activated T cells 1 (NFATc1), a master transcription factor for osteoclast differentiation. Collectively, our studies demonstrate a novel function of PDGF-D in the regulation of osteoclast activation, a key initial step for bone remodeling and the establishment of metastatic deposits of PCa cells at bone.

RESULTS

Prostate carcinoma-derived PDGF-D enhances tumor-take and growth rate at the skeletal sites

In order to examine the role of PCa-produced PDGF-D on tumor growth within bones, LNCaP-neo and PDGF-D-expressing LNCaP cells (LNCaP-PDGF-D) were injected into tibiae of male severe combined immunodeficient mice. LNCaP cells are known to grow poorly within the bone environment. However, radiographic analyses showed visible signs of bone reactions in a majority of tibiae injected with LNCaP-PDGF-D cells after 11 weeks (data not shown). Radiographic analyses after 17 weeks revealed significant bone reactions in the majority of mice injected intratibially with LNCaP-PDGF-D cells. In contrast, only one mouse injected intratibially with LNCaP-neo cells showed signs suggestive of changes in bone structure (Figure 1a). After 18 weeks, mice were killed and histopathological examinations of tibiae confirmed intraosseous tumor growth in the tibiae with radiographic changes. As graphed in Figure 1b, 8 out of 13 tibiae injected with LNCaP-PDGF-D harbored intraosseous tumors, whereas only 1 out of 14 tibiae injected with LNCaP-neo cells contained intraosseous tumor. In tibiae harboring LNCaP-PDGF-D tumors, the majority of the bone marrow cavity was replaced by PCa cells, where 10–60% of the residual bone surface was found to be adjacent to tumor cells. In contrast, $<5\%$ of the bone surface interacted with LNCaP-neo tumor cells. Bone histomorphometric analysis showed that the average tumor area (pixels^2) of LNCaP-PDGF-D tumors was 6 049 937, as compared with 469 718 in the one bone tumor formed by LNCaP-neo cells (Figure 1c). These results demonstrated that PDGF-D expression drastically increased both tumor take and intraosseous growth of LNCaP cells in the bone microenvironment.

Prostate carcinoma-derived PDGF-D induces pronounced bone stromal responses

Histopathological analyses of intraosseous LNCaP-PDGF-D tumors displayed both osteolytic and osteoblastic reactions, revealing a

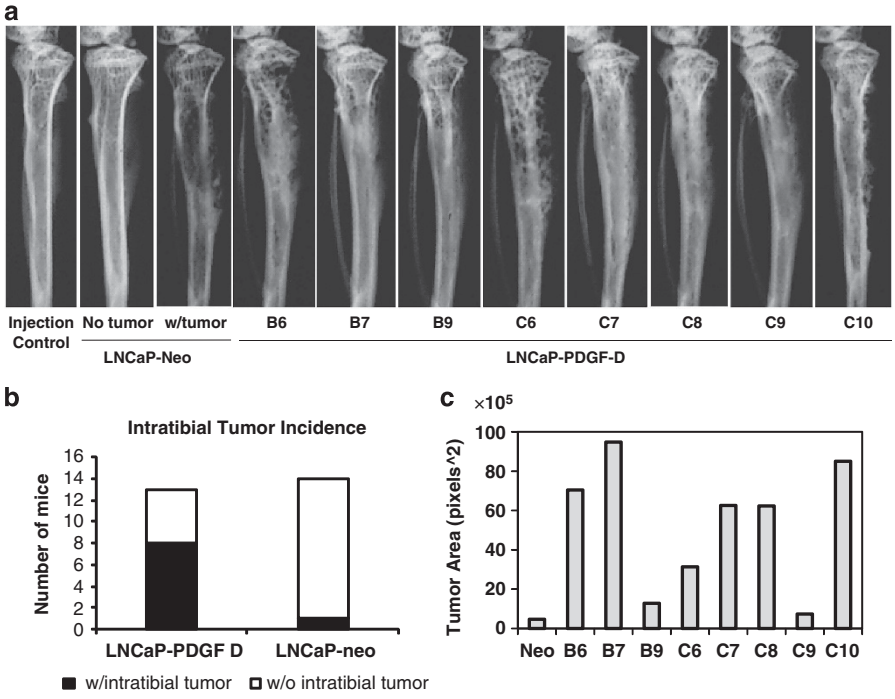

Figure 1. Prostate carcinoma-derived PDGF-D enhances bone reactions and intraosseous tumor growth. (**a**) Radiographic images of tibiae taken 17 weeks post-injection include a tibia injected with medium only (Injection control), one tibia injected with LNCaP-neo cells without tumor development (LNCaP-neo, no tumor), the only tibia of this group with intraosseous tumor growth (LNCaP-neo, w/tumor) and 8 tibiae bearing intraosseous LNCaP-PDGF-D tumors (mice B6, B7, B9, C6, C7, C8, C9, C10). The only LNCaP-neo tumor-bearing tibiae showed osteolytic appearance on its upper half with profound loss of bone trabecular and thinner bone cortex. LNCaP-PDGF-D bearing tibiae showed a mixed bone response. (**b**) Skeletal tumor incidence: number of mice with or without intraosseous tumor growth after injection with LNCaP-neo or LNCaP-PDGF-D cells (although 15 mice were injected in each group, two PDGF-D mice and one neo mouse died prematurely). (**c**) Skeletal tumor burden: tumor areas in the histological section of the entire tibia were calculated on the basis of the measurement of the corresponding areas in pixels^2 as described in Materials and methods.

keen resemblance to human prostate bone metastases.[13] In Figure 2a, hematoxylin and eosin (H&E) staining of tumor-bearing bones revealed that the LNCaP-PDGF-D tumor corresponding to No. C6 mouse tibiae (Figure 1a) formed a big tumor mass in the bone marrow cavity. The intratibial LNCaP-PDGF-D tumor was in close proximity to abundant woven bone with densely deposited bone matrix that was shown as dark blue color (collagen I) by trichrome staining. The activated osteoclastic cells, manifested by the dark purple color with Tartrate Resistant Acid Phosphatase (TRAP) staining, were distributed almost exclusively at the woven bone interface with LNCaP-PDGF-D tumors (arrows in Figure 2a). Osteoclast activation was readily detected in all intratibial LNCaP tumors as shown in Supplementary Figure 1. In contrast, the intraosseous LNCaP-neo tumor only formed three tiny tumor islands throughout the whole tibia section. A typical LNCaP-neo tumor island was shown in Figure 2b, which was circled by the

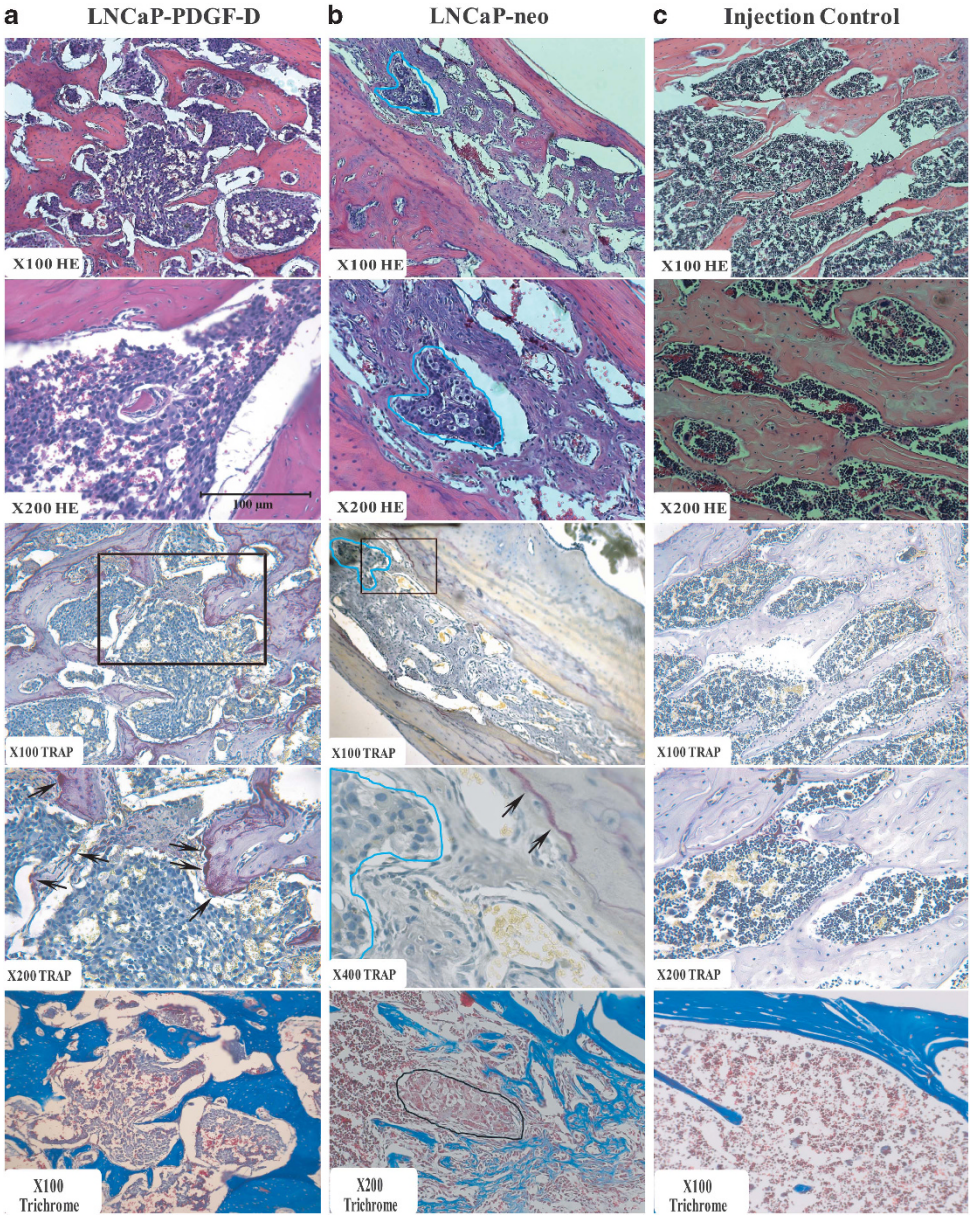

Figure 2. LNCaP-derived PDGF-D induces pronounced osteoclastic and osteoblastic responses. Sections of intraosseous LNCaP-PDGF-D tumor, LNCaP-neo tumor and control tibia injected with media only were analyzed by H&E, TRAP and trichrome staining, respectively. (**a**) LNCaP-PDGF-D tumor and its adjacent bone responses occupied the bone marrow cavity shown by H&E staining (× 100 HE and × 200 HE). The black-boxed area in TRAP staining (× 100 TRAP) was magnified to × 200 (× 200 TRAP). Activated osteoclast cells (arrows) at the LNCaP-PDGF-D tumor–bone interface were shown by the dark purple color by TRAP staining. The densely deposited collagen I in the woven bone was shown by the dark blue color by trichrome staining (× 100). (**b**) In H&E staining (× 100 and × 200), a small intraosseous LNCaP-neo tumor circled by blue lines is surrounded by a large sheet of osteoid. The black-boxed area in TRAP staining (× 100 TRAP) was magnified to × 400. TRAP staining showed very minor staining at the interface between osteoid and native trabecular bone (arrows). Trichrome staining showed that classic basophilic osteoblasts lined the interface between LNCaP-neo tumor (circled by black line) and neighboring osteoid tissue (light blue color). Many osteoblasts were embedded in the osteoid (light blue by trichrome staining) and turning into bone cells. (**c**) In H&E staining, the media injection-controlled tibia showed normal bone marrow tissue and intact native trabecular bone. TRAP staining showed little to no activated osteoclast cells within bone marrow tissue. Trichrome staining showed the native trabecular bone in dark blue color.

lines. Most interestingly, the tiny tumor island was surrounded by a massive sheet of osteoid, which was demonstrated by light blue color in trichrome staining. In addition, the LNCaP-neo tumor was adjacent to or lined by many basophilic osteoblastic cells shown by H&E staining. TRAP staining of LNCaP-neo tumor revealed a very minor osteoclastic response, which is at the interface between the osteoblastic response and native trabecular bone, but not adjacent to the LNCaP-neo tumor. Histopathological analyses of tibia from injection control showed intact native trabecular bones and normal bone marrow tissue (Figure 2c), where little to no TRAP staining is observed at the interface between bone marrow and trabecular bone. Trichrome staining showed dark blue color in the native trabecular bone. Taken together, these results suggest that the PDGF-D-mediated bone reactions, especially osteoclast activation, are critical for early onset, effective growth and expansion of the tumor deposit of human PCa LNCaP cells in the bone microenvironment.

PDGF-D, but not PDGF-B, induces osteoclastic differentiation *in vitro* independent of RANKL/RANK pathway

On the basis of the above results, we hypothesized that PDGF-D mediates osteoclastic differentiation critical for the establishment and expansion of intraosseous tumor growth. To test this hypothesis, we chose the mouse preosteoclast cell line RAW264.7 as an *in vitro* model. RT–PCR analysis of RNA obtained from RAW264.7 cells showed low mRNA expression of β-PDGFR and a non-detectable level of α-PDGFR, as compared with NIH3T3 cells (Figure 3a). As previously reported,[14] RAW264.7 cells express urokinase-type plasminogen activator, an activator of PDGF-D.[5]

To confirm that full-length rPDGF-D can be processed by proteinase(s) produced by RAW264.7 cells, rPDGF-D was incubated with conditioned medium (CM) collected from RAW264.7 cells or serum-free medium (negative control). As shown in Figure 3b, rPDGF-D was effectively processed into the 18kDa active GFD by RAW264.7-derived proteinase(s) in a time-dependent manner. To determine whether PDGF-D directly regulates osteoclastic differentiation, and if so, whether PDGFR activation by PDGF-B has similar effects, RAW264.7 cells were treated with rPDGF-D or rPDGF-B dimers at the same molar concentration. The osteoclastogenic factor RANKL was included as a positive control,[15,16] while dulbecco's modified eagle's medium (DMEM) containing 0.5% fetal bovine serum (FBS) was used as a negative control. As shown in Figure 3c, rPDGF-D effectively induced the differentiation of the pre-osteoclast cells, as detected by multinucleation and positive TRAP staining. The number of differentiated osteoclasts increased upon PDGF-D or RANKL treatments in a dose-dependent manner (Figure 3d). Real-time PCR analysis showed increased TRAP expression at the mRNA level upon treatments with PDGF-D or RANKL (Figure 3e). In contrast, PDGFR activation by PDGF-B failed to induce osteoclast differentiation or TRAP mRNA expression in these cells (Figures 3c–e). While PDGF-D effectively induced osteoclastic differentiation at a concentration of 10 ng/ml, PDGF B failed to induce osteoclast differentiation even at a concentration of 40 ng/ml (Figure 3d).

To ensure that both PDGF ligands used in these experiments were biologically active, rPDGF-B and rPDGF-D were applied to serum-starved NIH3T3 cells for 10 min, followed by the analysis of β-PDGFR activation. PDGF-B activated β-PDGFR more effectively than PDGF-D in NIH3T3 cells (Figure 3f), consistent with previous

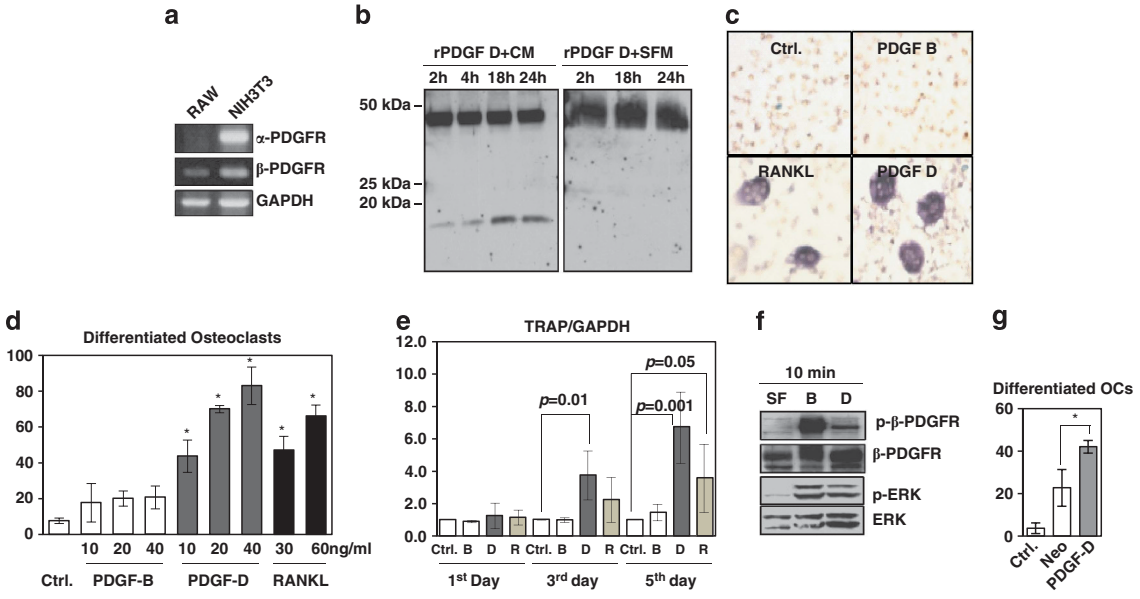

Figure 3. PDGF-D induces osteoclast differentiation *in vitro*. (**a**) RT–PCR analysis of α-PDGFR and β-PDGFR mRNA in RAW264.7 and NIH 3T3 cells. (**b**) Full-length rPDGF-D was incubated with CM collected from RAW264.7 cells (left panel) or with serum-free medium (right panel). At indicated time points, the processing of rPDGF-D was assessed by immunoblot analysis in a reducing condition using anti-PDGF-D antibody (8D2). (**c**) TRAP staining of RAW264.7 cells treated with 12.5 ng/ml (0.5 nM) rPDGF-B, 30 ng/ml (1.5 nM) rRANKL or 40 ng/ml (0.5 nM) rPDGF-D for 6 days. Note that RANKL exists as a monomer and yet works as a trimer while binding with RANK on cell surface. Pictures were taken under ×400 magnification. (**d**) RAW264.7 cells were treated with indicated concentration of PDGF-B, PDGF-D and RANKL for 6 days. An average number of differentiated osteoclast cells defined as TRAP-positive multinucleated cells (more than three nuclei/cell) in five low-power fields per treatment is shown. $*P<0.01$. (**e**) RAW264.7 cells were treated with 12.5 ng/ml (0.5 nM) PDGF-B, 40 ng/ml (0.5 nM) PDGF-D and 30 ng/ml (1.5 nM) RANKL for indicated days. The fold induction of TRAP mRNA normalized to the GAPDH level at indicated time points is graphed. TRAP mRNA level in control group (containing 0.5% FBS) was given as 1. Statistical analyses were based on three independent experiments performed in triplicates. *P* values were labeled between groups. (**f**) NIH3T3 cells were treated with 0.5 nM rPDGF-B (12.5 ng/ml) or rPDGF-D (40 ng/ml, activated by matriptase) for 10 min. The levels of p-β-PDGFR, β-PDGFR, pERKs and ERKs were analyzed by immunoblot analyses. (**g**) RAW264.7 cells were treated with concentrated CM from LNCaP-neo and LNCaP-PDGF-D cells for 6 days followed by TRAP staining. An average number of differentiated osteoclast cells by each treatment were graphed. $*P<0.01$.

reports that PDGF-B is a stronger agonist for β-PDGFR than PDGF-D.[17] Extracellular signal-regulated kinases, downstream signaling molecules of PDGFR, were also activated in NIH3T3 cells, confirming that both rPDGF-B and rPDGF-D are biologically active.

We previously showed that LNCaP cells auto-activate latent PDGF-D into the active form that can induce phosphorylation of β-PDGFR in a paracrine manner.[12] Importantly, CM from LNCaP-PDGF-D cells induced a significant increase in osteoclast differentiation *in vitro* compared with CM from LNCaP-neo control cells (Figure 3g).

It was previously shown that increased expression and nuclear translocation of NFATc1, the master transcription factor for osteoclastogenesis, is a key event for osteoclast differentiation.[18–20] Therefore, we examined the levels of NFATc1 in RAW264.7 cells following the treatment with rPDGF-B, rPDGF-D and rRANKL. As shown in Figure 4a, markedly increased NFATc1 staining was observed in multinucleated RAW264.7 cells following RANKL or PDGF-D treatment, but not PDGF-B treatment. Immunoblot analysis of NFATc1 showed that RANKL increases the nuclear NFATc1 level, in agreement with previous reports.[18,19] Importantly, PDGF-D, but not PDGF-B, drastically increased expression levels of NFATc1 especially in the nuclear fraction (Figure 4b, top panel), further supporting a novel function of PDGF-D in the regulation of osteoclast differentiation. As controls of cytoplasmic and nuclear fractions, the same blot was probed with GAPDH and histone H1 antibodies (Figure 4b, middle and bottom panels). To assess the functional significance of NFATc1 in PDGF-D-mediated osteoclast activation, preosteoclast cells were treated with rPDGF-D in the presence or absence of 0.3 μM NFAT inhibitor. Expression of osteoclast differentiation marker TRAP was significantly reduced in the presence of NFATc1 inhibitor, demonstrating a critical role for NFATc1 in PDGF-D-mediated osteoclast differentiation (Figure 4c). We next asked whether PDGF-D-mediated osteoclast differentiation involves RANKL/RANK pathway. When the effects of PDGF-D on RANKL expression were examined at the protein and RNA levels, neither the immunoblot nor the RT–PCR analysis detected RANKL expression with or without PDGF-D treatments (data not shown), suggesting that PDGF-D induction of RANKL/RANK autocrine signaling is unlikely in RAW264.7 cells. To further investigate the possible involvement of RANKL/RANK signaling, RANKL- and PDGF-D-induced osteoclast differentiation were examined in the presence or absence of osteoprotegerin, a soluble decoy receptor for RANKL.[15,21] As expected, osteoprotegerin effectively abolished the RANKL-induced osteoclastic differentiation. In contrast, it had little effect on PDGF-D-induced osteoclastogenesis (Figure 5). Taken together, these results unveiled a novel function of PDGF-D in the regulation of osteoclast differentiation utilizing a novel signaling pathway independent of RANKL/RANK interactions.

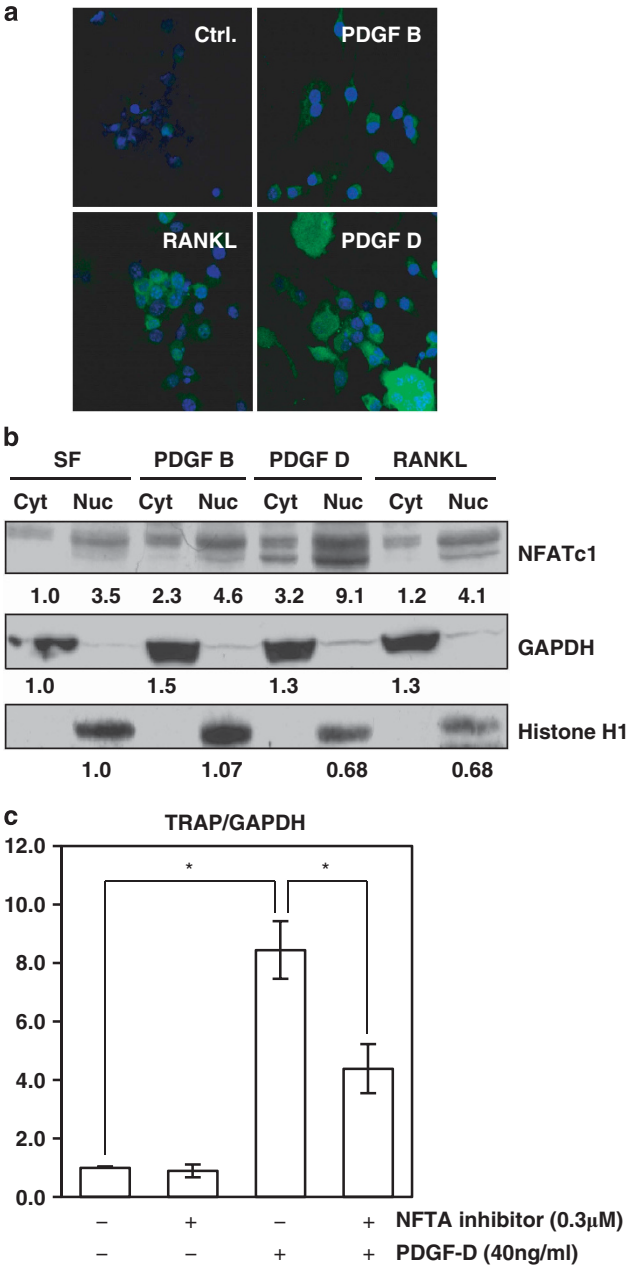

Figure 4. PDGF-D induced osteoclast differentiation is NFAT dependent. (**a**) Immunofluorescent staining of NFATc1 in RAW264.7 cells after treatments for 24 h with 12.5 ng/ml PDGF-B, 40 ng/ml PDGF-D or 20 ng/ml RANKL. (**b**) Immunoblot analysis of cytoplasmic (Cyt) and nuclear (Nuc) fractions of NFATc1 in RAW264.7 cells after different treatments for 72 h. The same blot was reprobed with anti-histone H1 and GAPDH antibodies as controls for nuclear and cytoplasmic fractions, respectively. Densitometry of target bands was quantitated using Image J software, and the cytoplasmic and nuclear NFATc1 protein levels were normalized to GAPDH and histone H1, respectively. The NFATc1 band in the cytoplasmic fraction in serum-free condition was given as 1. (**c**) RAW264.7 cells were treated with recombinant PDGF-D (40 ng/ml) in the presence or absence of NFTA inhibitor III 0.3 μM for 5 days. The relative levels of TRAP mRNA over GAPDH mRNA after treatments were graphed. Statistical analyses were based on three independent experiments performed in triplicates. $^*P < 0.01$.

Proteolytic processing of PDGF-D at the hinge region is essential for its biological activity to induce osteoclastic differentiation

We previously identified the arginine residues (R247 and R249) in the hinge region to be critical for the proteolytic processing of PDGF-D into HD and GFD-D by serine proteases such as urokinase-type plasminogen activator and matriptase.[5,6] Next, we asked whether proteolytic processing of PDGF-D at the hinge region is crucial to its osteoclastic effect on RAW264.7 cells. To address this question, RAW264.7 cells were treated with wild-type (WT) or the cleavage-deficient PDGF-D mutant proteins, followed by TRAP staining and real-time RT–PCR analysis of TRAP mRNA. As shown in Figure 6, the cleavage-deficient PDGF-D mutant proteins failed to induce osteoclast activation and TRAP expression (Figure 6), further supporting our conclusion that the proteolytic processing of full-length PDGF-D is required for PDGF-D activation of preosteoclasts. Lastly, we provide *in vivo* evidence that β-PDGFR is present in activated osteoclasts as shown by β-PDGFR immunostaining and TRAP-positive multinucleated cells utilizing adjacent sections of mouse tibiae (Figure 7).

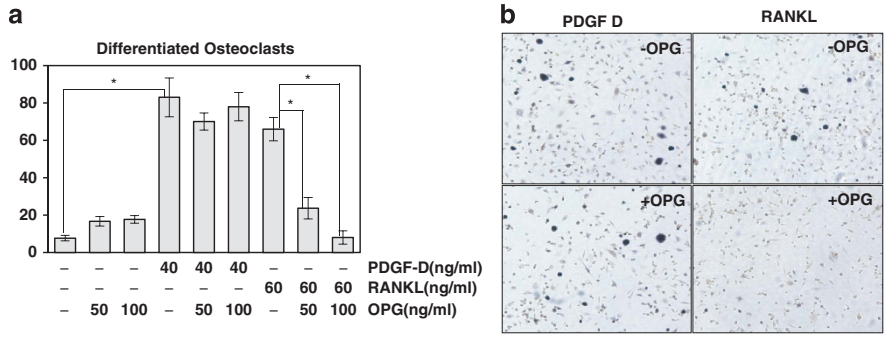

Figure 5. Osteoprotegerin has little effect on PDGF-D-induced osteoclast differentiation. (**a**) RAW264.7 cells were treated with 60 ng/ml RANKL or 40 ng/ml PDGF-D in the presence or absence of 50 or 100 ng/ml osteoprotegerin (OPG) for 6 days. An average number of TRAP positive multinucleated cells (more than three nuclei/per cell) in five low-power fields per glass cover slip is shown. $^*P<0.01$. (**b**) Representative pictures taken after each treatment.

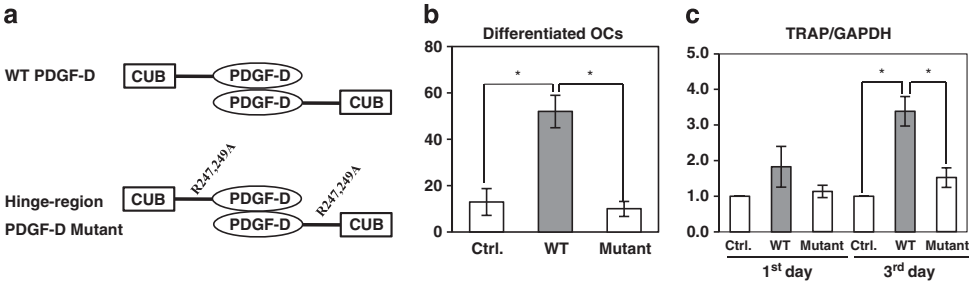

Figure 6. Processing of full-length PDGF-D is required for the induction of osteoclastic differentiation in RAW264.7 cells. (**a**) Diagrams of WT or hinge-region mutant (R247, 249A) PDGF-D dimers. (**b**) RAW264.7 cells were treated with concentrated CM containing WT or mutant PDGF-D for 6 days followed by TRAP staining. Average numbers of differentiated osteoclast cells of treatments were graphed. $^*P<0.01$. (**c**) RAW264.7 cells were treated with CM containing WT or mutant PDGF-D for 3 days. Relative levels of TRAP mRNA after treatments were analyzed by real-time PCR against GAPDH. $^*P<0.01$.

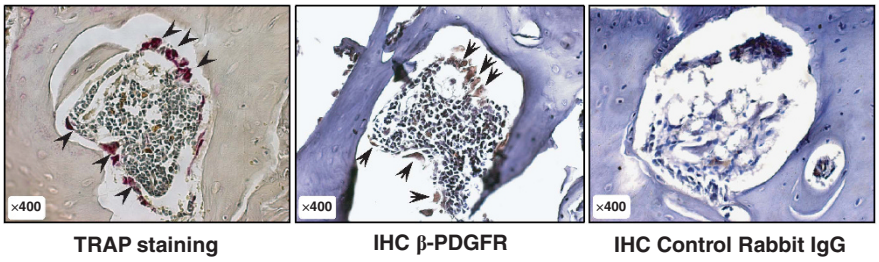

Figure 7. Activated osteoclasts express PDGFR-β. TRAP staining and immunohistochemistry staining of β-PDGFR were performed on adjacent mouse tibiae slides. Activated osteoclast cells shown by TRAP staining (arrows on left panel) express β-PDGFR shown by immunohistochemistry staining (arrows on middle panel). Control rabbit IgG was used as a negative control for β-PDGFR IHC in osteoclasts (right panel). Meyer's hematoxylin was used to counterstain nuclei. Images were taken at magnification $\times 400$.

DISCUSSION

A significant proportion of PCa patients develop metastatic disease after local therapy, with growth and expansion of skeletal tumor deposits, the leading cause of morbidity and mortality in this disease.[22] PCa bone metastases are generally categorized as osteoblastic, based on radiographic imaging. However, on a cellular level, most patients have components of both bone resorption and bone formation. Both clinical and experimental data supports a pivotal role of osteoclasts in the pathogenesis of cancer bone metastasis, regardless of the radiographic appearance.[23] Osteoclastic activation is believed to be a key initiator of bone metastasis for PCa, followed by the release of numerous growth factors from bone matrix in favor of tumor growth and the establishment of bone metastasis. Osteoclastic bone resorption is elevated in bone metastases from many different types of cancer, causing skeletal-related complications such as bone pain, hypercalcemia, pathological bone loss, and spinal cord and nerve compression syndromes. In this regard, our finding of a novel role of PDGF-D in osteoclast activation may not only help us understand the molecular mechanisms of PCa bone metastasis, but also may have broad implications in many human diseases.

Although recent studies indicated increased β-PDGFR signaling in PCa bone metastasis, knowledge in this area remains incomplete. The present study demonstrates that tumor-produced PDGF-D mediates both osteoclastic and osteoblastic reactions *in vivo*. Consistent with our findings, recent clinical trials in patients with either chronic myelogenous leukemia or gastrointestinal stromal tumors who received imatinib mesylate

predicted critical roles of PDGF receptor signaling in both bone resorption and bone formation.[24,25] In fact, previous studies over recent decades have suggested molecular mechanisms by which PDGF, a mesenchymal growth factor, regulates the bone turnover process. PDGF regulates the commitment of stromal mesenchymal cells to differentiate into osteoprogenitor cells,[26–28] suggesting a role for PDGF in bone formation. In addition, PDGF was thought to stimulate bone resorption by upregulating matrix-degrading enzyme expression.[29–31] However, neither the PDGF ligand-specific β-PDGFR signaling cascade nor a direct role for PDGF signaling in osteoclast activation has been reported. In this regard, our novel finding that PCa-derived PDGF-D induces osteoclast activation is of importance. It is also echoing the *in vivo* study by Uutela *et al*.[32] where PDGF-D induced remarkable recruitment of macrophages during the process of wound healing in PDGF-D transgenic mice, implicating the role of PDGF-D in cells from the monocytic lineage. While PDGF-B undergoes intracellular proteolytic processing and is secreted as an active growth factor, PDGF-D undergoes extracellular proteolytic processing to gain its biological activity. Here, we provided evidence that a novel function of PDGF-D in stimulating preosteoclasts also requires sequential processing of the latent PDGF-D into an active form by extracellular proteases. The present study revealed striking differences between two β-PDGFR activators, PDGF-B and PDGF-D, in mediating signal transduction. This finding is likely to have broad implications in many cellular processes regulated by PDGF-B and PDGF-D. Our study may also provide valuable information for the design of better therapeutic agents targeting the PDGF-D/β-PDGFR axis, rather than using selective, but not specific, tyrosine kinase inhibitors, such as imatinib mesylate, that showed only limited success in PCa patients at least in part due to side effects such as irritation in gastrointestinal tract and cardiotoxicity.[33–35]

The CUB domain of PDGF-D prevents its GFD from binding and activating its cognate receptor, β-PDGFR. Our recent study demonstrated that serine proteases, such as urokinase-type plasminogen activator and matriptase, process the full-length PDGF-D dimer into the GFD-D in a two-step manner involving the generation of HD, an intermediate dimer species containing one full-length and one GFD.[6] Consistent with our data that the CUB domain is involved in modulating the biological activity of PDGF-D, a recent study showed that cells expressing full-length PDGF-D are more tumorigenic *in vivo* than those expressing activated GFD alone.[36] The present study also suggests the potential significance of PDGF-D-specific signaling capacity in a cell-type-specific manner during PCa progression. The present study demonstrated that tumor-produced PDGF-D mediates bone reactions and enhances LNCaP tumor growth in the bone microenvironment. When LNCaP-neo and LNCaP-PDGF-D cells were subcutaneously injected, PDGF-D expression had little effect on either tumorigenicity or tumor volumes, whereas PDGF-D drastically enhances PCa interactions with surrounding stromal cells.[12] Taken together, we propose that PDGF-D-mediated stromal interactions are critical for PCa tumor expansion in the bone microenvironment, as the normal bone matrix is not conductive to tumor cell colonization. In contrast, PDGF-D-mediated tumor–stromal interactions may be critical for tumor cell invasion/metastasis and less critical for tumor growth in the primary site. Moreover, the present study demonstrated, for the first time, a novel osteoclast-inducing role of PDGF-D, independent of RANK/RANKL. These results open up new avenues for bone-specific targeted therapies in PCa bone metastasis and may have important implications with regard to osteoclast biology in general.

MATERIALS AND METHODS

Cell culture and reagents

The establishment and maintenance of control and PDGF-D transfected LNCaP cells were described previously.[12] Monocytic RAW264.7 cells were purchased from ATCC (Manassas, VA, USA) and maintained in DMEM with 10% FBS (HyClone, Logan, UT, USA). NIH3T3 mouse fibroblasts were maintained in DMEM/F12 medium supplemented with 10% bovine serum (Invitrogen, Carlsbad, CA, USA). Recombinant RANKL and PDGF-B proteins were purchased from Peprotech Inc. (Rocky Hill, NJ, USA) and Calbiochem (Gibbstown, NJ, USA), respectively. Recombinant PDGF-D was generated using the vaccinia expression system[12] and purified using His-Trap column from Amersham Biosciences (Piscataway, NJ, USA) following manufacturer's instruction. The quality and concentration of purified recombinant PDGF-D was determined on the basis of silver staining using SilverSNAP staining kit from Thermo Scientific (Rockford, IL, USA). NFATc1 antibodies for immunoblot analysis and immunofluorescence were purchased from BD Biosciences (Franklin Lakes, NJ, USA) and Santa Cruz Biotechnology Inc. (Santa Cruz, CA, USA), respectively. Histone H1 antibody was purchased from Millipore (Billerica, MA, USA). All other antibodies were purchased from Cell Signaling Biotechnology Inc. (Danvers, MA, USA). NFAT inhibitor III was purchased from Calbiochem (Gibbstown, NJ, USA).

Intratibial injection of LNCaP cells

Five-week-old male CB-17 severe combined immunodeficient mice were purchased from Taconic Farms (Germantown, NY, USA). In order to model the expanding metastatic deposit, 2×10^5 LNCaP-PDGF-D and LNCaP-neo cells were injected into the proximal end of tibiae 4–5 mm down the diaphysis. A total of 15 mice were used for each group and 4 mice were injected with medium as a control. Lukens bone wax (Surgical Specialties Co., Reading, PA, USA) was applied over the injection site to prevent cell leakage. Starting from the third week, mice were monitored by X-rays bi-weekly. All procedures were done in compliance with the Animal Investigation Committee of Wayne State University and NIH guidelines.

Histomorphometry

After 18 weeks, tibiae were harvested, X-rayed, fixed with 4% paraformaldehyde for 24 h, decalcified in 10% EDTA for 10–14 days and paraffin embedded. The bone tissues were sectioned longitudinally across the bone marrow cavity with a thickness of 5 μm and stained with H&E. Representative slide of each tibial sample was selected by a pathologist for analyzing tumor area. Digital photomicrographs were captured under × 5 magnification using a Zeiss Axioplan 2 microscope (Zeiss, Göttingen, Germany) equipped with a software-controlled digital camera (Axiovision; Zeiss); images were merged to display a panoramic view of the entire sagittal section of the tibia. The area occupied by the tumor in the histological section was calculated by the software based on the measurement of the corresponding areas in pixels,[2] as described previously,[37] which was shown as a bar graph for each tumor-bearing tibia in Figure 1c.

TRAP staining of tibiae bone sections

TRAP staining was performed using an acid phosphatase leukocyte kit from Sigma Aldrich (St Louis, MO, USA) per the manufacturer's protocol. Activated osteoclasts were detected as TRAP-positive multinucleated cells with dark purple staining in the cytoplasm.

Masson's trichrome staining

Trichrome staining was performed using Trichome Staining kit from Sigma Aldrich following manufacturer's protocol. The cytoplasma was stained in red and the collagen I was stained as blue.

Immunohistochemical staining of β-PDGFR

Immunohistochemical staining of β-PDGFR was performed on formalin-fixed, paraffin-embedded mouse tibiae slides. Antigen retrieval was performed by using sodium citrate buffer (pH 6.5). Slides were incubated with anti-β-PDGFR antibody (Calbiochem, cat# PC17, 1:1000) at 4°C overnight and visualized with DAB (Vector Labs, Burlingame, CA, USA). Negative controls were performed using rabbit IgG (Cat# I-1000, 1:1000, Vector Labs). Meyer's hematoxylin purchased from SycTek Laboratories, Inc. (Logan, UT, USA) was used to counterstain nuclei.

In vitro differentiation of preosteoclast-like RAW264.7 cells

RAW264.7 cells (1×10^5/well), grown on glass coverslips in a 12-well plate, were treated with rPDGF-B, rPDGF-D or RANKL at indicated concentrations in DMEM containing 0.5% FBS. Each treatment was performed in triplicate and the medium was refreshed every 2 days. After 6 days, cells were fixed with 4% paraformaldehyde, and TRAP staining was performed as described above. Activated osteoclasts, detected as TRAP-positive multinucleated cells (more than three nuclei/cell), were counted in five randomly selected fields examined at $\times 100$ magnification using a Zeiss Axioplan 2 microscope.

Real-time RT–PCR analysis

Total RNA was isolated from RAW264.7 cells at indicated time points using RNeasy Mini Kit (Qiagen, Valencia, CA, USA). The cDNA was synthesized using iScript cDNA synthesis kit (Bio-Rad, Hercules, CA, USA) according to manufacturer's instruction. Real-time PCR was performed using Brilliant QPCR Master Mix (Stratagene, La Jolla, CA, USA), and triplicate samples were run in the *Mx4000* Multiplex Quantitative PCR system (Stratagene) and analyzed using the 2^{-CT} method. Each experiment was repeated at least three times. Statistical analyses were based on at least three individual experiments. The forward and reverse primers for TRAP are 5′-TCTCTGGGGGACAATTTCTA-3′ and 5′-CTGACTGGCAAAGTCATCTG-3′, respectively. GAPDH is used as the internal control. The forward and reverse primers for GAPDH are 5′-ATCACCATCTTCCAGGAGCGA-3′ and 5′-GCCAGTGAGCTTCCCGTTCA-3′, respectively.

Fractionation of nuclear and cytoplasmic proteins

RAW264.7 cells were treated with 1 nM rRANKL, 0.5 nM rPDGF-B or 0.5 nM rPDGF-D in serum-free DMEM for 3 days. Cells were sequentially lysed with cytoplasmic lysis buffer (25 mM HEPES pH 7.8, 10 mM KCl, 1.5 mM MgCl2, 0.5% NP-40, protease inhibitor cocktail (Sigma Aldrich), 0.1 M dithiothreitol, 100 mM PMSF) and nuclear lysis buffer (50 mM HEPES pH7.9, 140 mM NaCl, 1 mM EDTA, 1% triton X-100, 0.1% sodium deoxycholate, protease inhibitor cocktail, 0.1 M dithiothreitol and 100 mM PMSF) on ice. Cytoplasmic and nuclear proteins in the supernatant were collected and analyzed by immunoblotting, respectively. Densitometry of protein bands was determined using software Image J from National Institute of Health (Bethesda, MD, USA).

Immunofluorescent staining

RAW264.7 cells, grown on chamber slides (Nalge Nunc International, Naperville, IL, USA) at 50% confluency overnight, were fixed with 4% paraformaldehyde and permeabilized with 0.5% Triton X-100 at 4 °C for 10 min. After blocking, cells were stained with primary antibodies and fluorescein isothiocyanate -conjugated secondary antibody (Jackson Immunoresearch Laboratories, West Grove, PA, USA). The nuclei were stained with DAPI. The slides were then mounted with anti-fade solution (Invitrogen), followed by immunofluorescence microscopic analysis using the Zeiss LSM510 confocal microscopy system with a $\times 40$ lens (NA = 1.3).

Generation of concentrated CM from LNCaP-neo and LNCaP-PDGF-D cells

Equal numbers of LNCaP-neo and LNCaP-PDGF-D cells were seeded into plastic plates. On the following day, cells were serum starved for 48 h before CM was collected. CM were concentrated against PBS four times using Amicon Ultra centrifuge filters from Millipore. Concentration of concentrated CM was determined by bicinchoninic acid assay.

Generation of WT PDGF-D and hinge-region mutant PDGF-D

WT and mutant PDGF-D were generated through the vaccinia virus system by infect/transfect CV-1 cells with vTF-7 virus and pTF-7–PDGF-D plasmids. After 18 h, CM containing WT or hinge-region mutated PDGF-D was collected and concentrated against PBS as described above.

Statistical analysis

A nonpaired Student's *t*-test was used for comparison between two groups. $P < 0.05$ was considered statistically significant. Statistical analyses were based on three independent experiments performed in triplicates. *P* values were labeled between groups.

CONFLICT OF INTEREST

The authors declare no conflict of interest.

ACKNOWLEDGEMENTS

This work was supported by NIH/NCI RO1 grants CA64139 and CA123362 (to H-RCK), R01CA137280 (to MLC) as well as the Ruth L. Kirschstein National Research Service Award T32-CA009531 (to MKC-L). We thank Dr. C-J Kim for his help with IHC analysis.

REFERENCES

1 Buijs JT, van der Pluijm G (2009) Osteotropic cancers: from primary tumor to bone. *Cancer Lett* **73**: 177 - 193.
2 Andrae J, Gallini R, Betsholtz C (2008) Role of platelet-derived growth factors in physiology and medicine. *Genes Dev* **2**: 276 - 312.
3 Reigstad LJ, Varhaug JE, Lillehaug JR (2005) Structural and functional specificities of PDGF-C and PDGF-D, the novel members of the platelet-derived growth factors family. *FEBS J* **272**: 5723 - 5741.
4 Fredriksson L, Li H, Fieber C, Li X, Eriksson U (2004) Tissue plasminogen activator is a potent activator of PDGF-CC. *EMBO J* **23**: 3793 - 3802.
5 Ustach CV, Kim H-RC (2005) Platelet-derived growth factor D is activated by urokinase plasminogen activator in prostate carcinoma cells. *Mol Cell Biol* **25**: 6279 - 6288.
6 Ustach CV, Huang W, Conley-LaComb MK, Lin CY, Che M, Abrams J *et al.* (2010) A novel signaling axis of matriptase/PDGF-D/ss-PDGFR in human prostate cancer. *Cancer Res* **70**: 9631 - 9640.
7 Chott A, Sun Z, Morganstern D, Pan J, Li T, Susani M *et al.* (1999) Tyrosine kinases expressed *in Vivo* by human prostate cancer bone marrow metastases and loss of the Type 1 insulin-like growth factor receptor. *Am J Pathol* **155**: 1271 - 1279.
8 Singh D, Febbo PG, Ross K, Jackson DG, Manola J, Ladd C *et al.* (2002) Gene expression correlates of clinical prostate cancer behavior. *Cancer Cell* **1**: 203 - 209.
9 Mathew P, Thall PF, Bucana CD, Oh WK, Morris MJ, Jones DM *et al.* (2007) Platelet-derived growth factor receptor inhibition and chemotherapy for castration-resistant prostate cancer with bone metastases. *Clin Cancer Res* **13**: 5816 - 5824.
10 Ng SS, MacPherson GR, Gutschow M, Eger K, Figg WD (2004) Antitumor effects of thalidomide analogs in human prostate cancer xenografts implanted in immunodeficient mice. *Clin Cancer Res* **10**(12 Pt 1): 4192 - 4197.
11 van der Poel HG (2004) Smart drugs in prostate cancer. *Eur Urol* **45**: 1 - 17.
12 Ustach CV, Taube ME, Hurst Jr NJ, Bhagat S, Bonfil RD, Cher ML *et al.* (2004) A potential oncogenic activity of platelet-derived growth factor d in prostate cancer progression. *Cancer Res* **64**: 1722 - 1729.
13 Roudier MP, Morrissey C, True LD, Higano CS, Vessella RL, Ott SM (2008) Histopathological assessment of prostate cancer bone osteoblastic metastases. *J Urol* **180**: 1154 - 1160.
14 Kubota K, Wakabayashi K, Matsuoka T (2003) Proteome analysis of secreted proteins during osteoclast differentiation using two different methods: two-dimensional electrophoresis and isotope-coded affinity tags analysis with two-dimensional chromatography. *Proteomics* **3**: 616 - 626.
15 Khosla S (2001) Minireview: the OPG/RANKL/RANK system. *Endocrinology* **142**: 5050 - 5055.
16 Blair JM, Zhou H, Seibel MJ, Dunstan CR (2006) Mechanisms of disease: roles of OPG, RANKL and RANK in the pathophysiology of skeletal metastasis. *Nat Clin Pract Oncol* **3**: 41 - 49.
17 LaRochelle WJ, Jeffers M, McDonald WF, Chillakuru RA, Giese NA, Lokker NA *et al.* (2001) PDGF-D, a new protease-activated growth factor. *Nat Cell Biol* **3**: 517 - 521.
18 Gohda J, Akiyama T, Koga T, Takayanagi H, Tanaka S, Inoue J (2005) RANK-mediated amplification of TRAF6 signaling leads to NFATc1 induction during osteoclastogenesis. *EMBO J* **24**: 790 - 799.
19 Takayanagi H, Kim S, Koga T, Nishina H, Isshiki M, Yoshida H *et al.* (2002) Induction and activation of the transcription factor NFATc1 (NFAT2) integrate RANKL signaling in terminal differentiation of osteoclasts. *Dev Cell* **3**: 889 - 901.
20 Wada T, Nakashima T, Hiroshi N, Penninger JM (2006) RANKL-RANK signaling in osteoclastogenesis and bone disease. *Trends Mol Med* **12**: 17 - 25.
21 Zhang J, Dai J, Qi Y, Lin DL, Smith P, Strayhorn C *et al.* (2001) Osteoprotegerin inhibits prostate cancer-induced osteoclastogenesis and prevents prostate tumor growth in the bone. *J Clin Invest* **107**: 1235 - 1244.

22 Mundy GR (2002) Metastasis to bone: causes, consequences and therapeutic opportunities. *Nat Rev Cancer* **2**: 584 - 593.
23 Taichman RS, Loberg RD, Mehra R, Pienta KJ (2007) The evolving biology and treatment of prostate cancer. *J Clin Invest* **117**: 2351 - 2361.
24 Berman E, Nicolaides M, Maki RG, Fleisher M, Chanel S, Scheu K *et al.* (2006) Altered bone and mineral metabolism in patients receiving imatinib mesylate. *N Engl J Med* **354**: 2006 - 2013.
25 Breccia M, Alimena G (2009) The metabolic consequences of imatinib mesylate: Changes on glucose, lypidic and bone metabolism. *Leuk Res* **33**: 871 - 875.
26 Chaudhary LR, Hofmeister AM, Hruska KA (2004) Differential growth factor control of bone formation through osteoprogenitor differentiation. *Bone* **34**: 402 - 411.
27 Godwin SL, Soltoff SP (1997) Extracellular calcium and platelet-derived growth factor promote receptor-mediated chemotaxis in osteoblasts through different signaling pathways. *J Biol Chem* **272**: 11307 - 11312.
28 Mehrotra M, Krane SM, Walters K, Pilbeam C (2004) Differential regulation of platelet-derived growth factor stimulated migration and proliferation in osteoblastic cells. *J Cell Biochem* **93**: 741 - 752.
29 Kubota K, Sakikawa C, Katsumata M, Nakamura T, Wakabayashi K (2002) Platelet-derived growth factor BB secreted from osteoclasts acts as an osteoblastogenesis inhibitory factor. *J Bone Miner Res* **17**: 257 - 265.
30 Himeno M, Enomoto H, Liu W, Ishizeki K, Nomura S, Kitamura Y *et al.* (2002) Impaired vascular invasion of Cbfa1-deficient cartilage engrafted in the spleen. *J Bone Miner Res* **17**: 1297 - 1305.
31 Robbins JR, McGuire PG, Wehrle-Haller B, Rogers SL (1999) Diminished matrix metalloproteinase 2 (MMP-2) in ectomesenchyme-derived tissues of the Patch mutant mouse: regulation of MMP-2 by PDGF and effects on mesenchymal cell migration. *Dev Biol* **212**: 255 - 263.
32 Uutela M, Wirzenius M, Paavonen K, Rajantie I, He Y, Karpanen T *et al.* (2004) PDGF-D induces macrophage recruitment, increased interstitial pressure, and blood vessel maturation during angiogenesis. *Blood* **104**: 3198 - 3204.
33 Deininger MW, Druker BJ (2003) Specific targeted therapy of chronic myelogenous leukemia with imatinib. *Pharmacol Rev* **55**: 401 - 423.
34 Guilhot F (2004) Indications for imatinib mesylate therapy and clinical management. *Oncologist* **9**: 271 - 281.
35 Kerkela R, Grazette L, Yacobi R, Iliescu C, Patten R, Beahm C *et al.* (2006) Cardiotoxicity of the cancer therapeutic agent imatinib mesylate. *Nat Med* **12**: 908 - 916.
36 Ehnman M, Li H, Fredriksson L, Pietras K, Eriksson U (2009) The uPA/uPAR system regulates the bioavailability of PDGF-DD: implications for tumour growth. *Oncogene* **28**: 534 - 544.
37 Bonfil RD, Dong Z, Trindade Filho JC, Sabbota A, Osenkowski P, Nabha S *et al.* (2007) Prostate cancer-associated membrane type 1-matrix metalloproteinase: a pivotal role in bone response and intraosseous tumor growth. *Am J Pathol* **170**: 2100 - 2111.

Supplementary Information accompanies the paper on the Oncogene website (http://www.nature.com/onc)